Searching for Ultralight Dark Matter with Optical Cavities

Andrew A. Geraci,[1] Colin Bradley,[2] Dongfeng Gao,[3] Jonathan Weinstein,[2] and Andrei Derevianko[2]
[1]Department of Physics and Astronomy, Northwestern University, Evanston, Illinois 60208, USA
[2]Department of Physics, University of Nevada, Reno, Nevada 89557, USA
[3]State Key Laboratory of Magnetic Resonance and Atomic and Molecular Physics, Wuhan Institute of Physics and Mathematics, Chinese Academy of Sciences, Wuhan 430071, China

(Received 1 August 2018; revised manuscript received 16 February 2019; published 17 July 2019)

We discuss the use of optical cavities as tools to search for dark matter (DM) composed of virialized ultralight fields (VULFs). Such fields could lead to oscillating fundamental constants, resulting in oscillations of the length of rigid bodies. We propose searching for these effects via differential strain measurement of rigid and suspended-mirror cavities. We estimate that more than 2 orders of magnitude of unexplored phase space for VULF DM couplings can be probed at VULF Compton frequencies in the audible range of 0.1–10 kHz.

DOI: 10.1103/PhysRevLett.123.031304

Introduction.—Despite overwhelming observational evidence for the existence of dark matter (DM), its composition and nongravitational interaction with standard model fields and particles remain a mystery [1–4]. Its presence is a strong indicator for new physics beyond the standard model, and among viable candidates are bosonic ultralight fields with masses below ∼10 eV, which behave as classical fields rather than individual particles (for a recent review see Ref. [5]). Such fields can be naturally produced in the early universe through the misalignment mechanism. We collectively refer to such candidates as VULFs (virialized ultralight fields).

One of the most well-motivated VULF candidates is a scalar field, motivated by string theory dilatons and moduli [6–11]. The multitude of topologically complex vacuua in string theory naturally leads to an abundance of moduli and dilatons. The values of parameters in the standard model such as the Yukawa couplings or the fine structure constant depend on the moduli fields. The moduli can acquire mass through supersymmetry (SUSY) breaking, and for TeV scale SUSY breaking the mass can be of order 0.1 meV [6]. Much lighter moduli masses are also possible due to loop factors and small coefficients, e.g., for the electron Yukawa modulus.

Such ultralight fields cause a time variation of fundamental constants such as the fine-structure constant α or the mass of the electron m_e [12]. A variety of experimental techniques have been used or proposed for VULF searches, including resonant cavities, torsion balances, atom interferometers, atomic clocks, molecular absorption, and magnetometers [13–21].

On timescales short compared to the VULF coherence time, the DM field can be expressed as

$$\phi(t,\mathbf{r}) \approx \frac{\hbar}{m_\phi c}\sqrt{2\rho_{\rm DM}}\cos\left[2\pi f_\phi t - \mathbf{k}_\phi\cdot\mathbf{r} + \cdots\right], \quad (1)$$

where $\rho_{\rm DM} \approx 0.4$ GeV/cm^3 is the local DM energy density, m_ϕ is the mass of the DM field, $f_\phi = m_\phi c^2/(2\pi\hbar)$ is the Compton frequency, and $k_\phi = m_\phi v/\hbar$ with v being the velocity of DM with respect to the instrument. Detailed discussion of the expected coherence properties of VULFs can be found in Ref. [22].

In the dilatonlike models, VULFs drive oscillations of the electron mass and fine structure constant,

$$\frac{\delta m_e(t,\mathbf{r})}{m_{e,0}} = d_{m_e}\sqrt{4\pi\hbar c}E_P^{-1}\phi(t,\mathbf{r}), \quad (2)$$

$$\frac{\delta\alpha(t,\mathbf{r})}{\alpha_0} = d_e\sqrt{4\pi\hbar c}E_P^{-1}\phi(t,\mathbf{r}). \quad (3)$$

Here d_{m_e} and d_e are dimensionless dilaton couplings and $E_P \equiv \sqrt{\hbar c^5/G}$ is the Planck energy. These effects could be searched for with atomic clocks and interferometers [13,15]; however, because of the finite interrogation time, they are limited to Compton frequencies of order 1 Hz and below. At higher frequencies, DM-induced strain in solids is a promising approach. The DM-induced oscillations (2), (3) of the fine structure constant and electron mass drive oscillations in the Bohr radius $a_0 = \hbar/(\alpha m_e c)$ and, therefore, in the size of atoms and chemical bonds. For sufficiently slow oscillation frequencies, this causes a time-varying strain h in solid materials, given by

$$h = -\frac{\delta\alpha}{\alpha_0} - \frac{\delta m_e}{m_{e,0}}, \quad (4)$$

where we have ignored small relativistic effects.

Previously, optical cavities have been proposed in searches for a coupling between axion DM and photons, using resonant enhancement from the cavity [23]. Here we propose to search for dilaton-DM-induced variations in

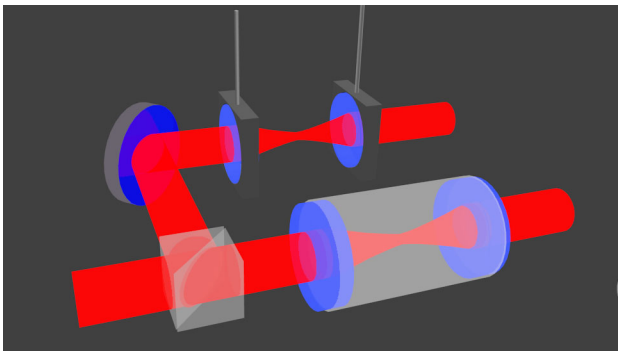

FIG. 1. Experimental setup. Light from a common laser is directed into two Fabry-Perot resonators, one with suspended mirror substrates and one with a rigid cavity spacer. Modulation in, e.g., the electron mass due to dilatonic DM at the 0.1–10 kHz frequency range results in periodic length changes in the rigid cavity, while the DM-induced length changes in the suspended interferometer are suppressed by the low frequency mechanical suspension.

fundamental constants by precisely measuring the resulting strain in optical cavities. Resonant bar detectors have also been proposed as a method of detecting ultralight-DM-induced strain in material bodies [19]. This approach relies on the resonant enhancement of the vibration of the bar relative to the surrounding objects, in order to differentiate the DM signal from the expansion and contraction of the remainder of the apparatus. Consequently, that approach is inherently a resonant method, with sensitivity significantly degraded off resonance. Here, we propose using two optical cavities—with different sensitivities to DM-induced strain—to search for the same signal. In contrast to bar detectors, the method we propose is *broadband*. Despite the lack of resonant enhancement, the Allan deviation of a laser locked to an optical cavity—superior to all other current technology at times $\lesssim 1$ s—is anticipated to extend the discovery reach for ultralight scalar field DM by up to 10^3 in the 0.1–10 kHz frequency band, corresponding to $m_\phi \approx 10^{-13}$–10^{-11} eV$/c^2$. Our method thus closes a gap in the mass range for VULF searches in the audible frequency band.

Proposed experiment.—We consider an arrangement of two colocated high-finesse Fabry-Perot optical cavities. The first optical cavity is constructed with mirrors connected by a rigid cavity spacer, as is typical for optical clocks. The second optical cavity consists of two mirrors suspended by pendulums, as is used in LIGO, with a resonant mechanical frequency below the frequencies of interest. This suppresses the sensitivity of the second cavity's length to high-frequency variations in the length of its supporting spacer. Thus, if the size of atoms oscillates in time, the length (and hence resonant frequency) of the first cavity should oscillate with respect to the second. The experimental technique described below essentially measures differential strain of the two cavities. The VULF signal would appear as a spike in the power spectral density (PSD) of the measured differential strain. The VULF signal is predicted [22] to exhibit a strongly asymmetric profile of width $\Delta f_\phi \approx 3 \times 10^{-6} f_\phi$. This distinct signature should allow us to discriminate the VULF signal from many conventional noise sources.

TABLE I. Experimental parameters chosen for the cavity with rigid spacer and suspended mirror cavity.

Parameter	Value	Description
L	30 cm	Cavity spacer length
$\mathcal{F}$	10^4	Cavity finesse
w	2 mm	Laser waist
λ	1550 nm	Laser wavelength
P	1 mW	Incident laser power
t	2 cm	Mirror substrate thickness
r	3 cm	Mirror substrate radius
d	4×10^{-6} m	Coating thickness
ϕ_c	2.7×10^{-4}	Loss angle coating
Φ	10^{-7}	Loss angle mirror substrate
$\phi_{\rm sp}$	10^{-6}	Loss angle spacer
$\phi_{\rm susp}$	2×10^{-7}	Loss angle suspension (> 1 kHz)
$d_{\rm wire}$	310 μm	Suspension wire diameter
$L_{\rm wire}$	8 cm	Suspension wire length
$R_{\rm sp}$	3 cm	Outer radius spacer
$r_{\rm sp}$	0.5 cm	Inner radius spacer
Y	70 GPa	Young's modulus, substrate and spacer
σ	0.25	Poisson ratio, substrate and spacer
Y_c	110 GPa	Young's modulus, coating
σ_c	0.22	Poisson ratio, coating
T	300 K	Cavity temperature

As shown in Fig. 1, light from a single laser is sent into both cavities. The cavities are located on a single optical table to suppress differential Doppler shifts of the laser light due to relative cavity motion. The laser frequency is locked to the first cavity using Pound-Drever-Hall (PDH) locking. PDH provides a high stabilization bandwidth not limited by the cavity response time [24]. The light traveling to the second cavity is frequency shifted onto resonance with the second cavity using an acousto-optic modulator (AOM). The frequency of the AOM is modulated to lock its transmitted light to the resonance of the second cavity using PDH. The AOM drive frequency is recorded directly (or mixed down to a lower frequency for lower-bandwidth recording), which provides the frequency shift $\Delta_f(t)$ of the resonant frequency of one cavity relative to the other as a function of time. The strain of one cavity relative to the other is simply $h(t) = \Delta_f(t)/f_0$, where f_0 is the nominal frequency of the laser. We consider three possible cavity lengths, of 10, 30, and 100 cm in order to provide coverage over the audible frequency band. While all cavities are broadband in detection, the choice of cavity length is a trade-off between strain sensitivity and maximum detectable frequency, as discussed below. The proposed experimental parameters are shown in Table I taking the 30 cm cavities as an example.

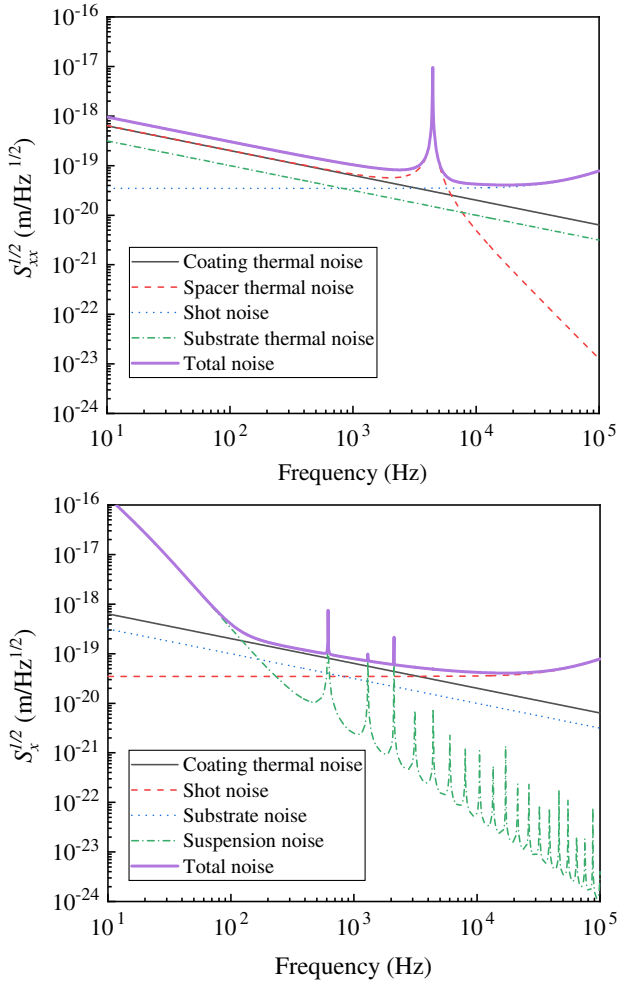

FIG. 2. Expected noise sources for the proposed experimental geometry, with parameters of Table I. Upper panel: cavity with rigid spacer. Lower panel: cavity with suspended mirror substrates.

The minimum detectable differential strain is limited by photon shot noise, as calculated below. However, the differential strain itself can originate not only from VULF DM, but also in technical noise sources, such as thermal fluctuations of the cavity spacers, the mirrors, and the mirror coatings. The limits that can be placed on VULF DM couplings are limited by these fluctuations as discussed below.

Noise sources and systematic effects.—There are several fundamental and technical sources of noise which limit the ability to measure the effective strain. A list of noise estimates are included in Fig. 2. In quantifying various noise sources, we operate in terms of one-sided displacement PSD $S_{xx}(f)$ related to the differential strain PSD as $S_{hh}(f) = S_{xx}(f)/L^2$, where L is the cavity length. The dominant sources of thermomechanical noise due to intrinsic dissipation tend to improve at higher frequency f as $f^{-1/2}$. Thus at frequencies above 10 kHz it is possible to realize shot-noise limited position detection. In the future, squeezed light offers the prospect for further improved sensitivity.

Photon shot noise limits the minimum detectable phase shift to $\delta\phi \sim 1/(2\sqrt{I})\sqrt{b}$, where $I = P/\hbar\omega_c$ is the incident photon flux from a laser of power P and frequency ω_c and b is the measurement bandwidth [25]. The corresponding photon shot-noise limited one-sided displacement PSD is $S_{xx}(f) = S_{xx,0}[1 + (2\pi f)/\Omega_{\rm cav}]$, for an impedance matched cavity of linewidth $\Omega_{\rm cav}$ [25]. Here $S_{xx,0} = (\lambda/16\mathcal{F}\sqrt{I})$, with $\mathcal{F}$ being the cavity finesse and λ the laser wavelength.

Coating thermal noise is a common limitation in precision optical cavity metrology both for the optical clock community and gravitational wave observatories [26]. Assuming similar coating and substrate mechanical parameters, we can arrive at a simplified expression for the noise [26,27]

$$S_{xx,\rm coat}(f) = \frac{2k_BT}{\pi^{3/2}f}\frac{1}{Y_c w(1-\sigma_c^2)}\phi_{\rm coat}, \tag{5}$$

where $\phi_{\rm coat} = (2d/\pi^{1/2}w)[(1-2\sigma_c)/(1-\sigma_c)]\phi_c$, for a coating at temperature T with Young's modulus Y_c, Poisson ratio σ_c, beam waist w, and coating loss angle parameter ϕ_c. Here, as in Ref. [27], we are assuming for simplicity that the coating properties are isotropic and we choose a multilayer dielectric stack of materials adding to thickness d and also assume a similar effective loss angle as in Ref. [27]. Our estimated coating noise level is about an order of magnitude less than that demonstrated in Ref. [27] because our chosen beam waist is nearly 10 times larger.

Spacer thermal noise in the rigid cavity contributes at a level similar to the mirror coatings for our experimental parameters. A simple harmonic oscillator in the low frequency regime has a spectral density [28]

$$S_{xx,\rm sp}(f) = \frac{4k_BTk\phi_{\rm sp}}{(2\pi f)\{[k-m(2\pi f)^2]2 + k^2\phi_{\rm sp}^2\}},$$

with k_B being Boltzmann's constant, T being the temperature, k being the effective spring constant, and $\phi_{\rm sp}$ being the loss factor of the material. For a homogeneous cylinder, the approximation of a simple harmonic oscillator is adequate. This assumption also yields the effective spring constant: $k = (YA/L)$ where Y is the Young's modulus of the material, A is the cross sectional area, and L is the length of the rod. For longitudinally driven oscillations near resonance, the effective mass is half the mass of the cylinder. The resulting spectral density is given in Fig. 2, which uses values for material properties for a silica spacer and silica or tantalum coatings [27,29]. These results could improve significantly using synthetic fused silica, as the loss factors can be much lower. In the low-frequency limit, for a cylinder of radius $R_{\rm sp}$ with a hole of radius $r_{\rm sp}$ bored through the center, the position spectral density due to thermal noise is given by the form [27]

$$S_{xx,\rm sp}(f) = \frac{4k_BT}{\pi f}\frac{L}{2\pi Y(R_{\rm sp}^2 - r_{\rm sp}^2)}\phi_{\rm sp}. \tag{6}$$

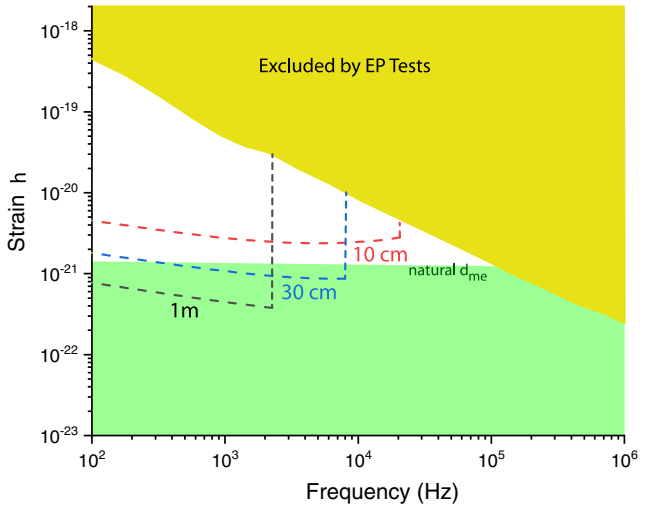

FIG. 3. Strain sensitivity of optical cavity limited by thermal noise for three cavity lengths as a function of VULF Compton frequency. Here we assume a total integration time of 10^7 s, with an improvement scaling with the averaging time τ as $\tau^{-1/2}$ up to the coherence time of the DM field ($\sim 10^6$ oscillations), and improving as $\tau^{-1/4}$ thereafter. Bounds from equivalence principle tests are shown as shaded yellow region [31,32]. Strains in the shaded green region are natural for an electron Yukawa modulus with a 10 TeV cutoff [19].

For the cavity consisting of freely suspended mirrors, the thermal noise in the wire suspension contributes in a manner similar to that in LIGO. We choose a fused silica single-wire suspension of length $L_{\rm wire}$, diameter $d_{\rm wire}$, and effective loss angle $\phi_{\rm susp}$ as specified in Table I, and study the pendulum, torsion, and violin modes assuming a modal approximation [30]. For $\phi_{\rm susp}$, we take a frequency dependent model as given in Ref. [30] which asymptotes to the value in Table I above $\sim$1 kHz. Apart from a few discrete narrow peaks corresponding to the violin modes, we expect the suspension noise to be subdominant to other thermal noise sources. For a realistic design, a tapered wire diameter may be chosen to further improve losses, as in LIGO [30].

The thermal Brownian motion of the mirror substrates takes the form [29]

$$S_{xx,\rm sub} = \frac{2k_BT}{\pi^{3/2} f}\frac{1}{Yw(1-\sigma^2)}\phi_{\rm sub}, \tag{7}$$

where σ is the Poisson ratio, and $\phi_{\rm sub}$ is the substrate loss angle. For the parameters considered, substrate thermal noise is expected to make a subdominant contribution to the total noise.

Current state-of-the-art optical cavities show many more mechanical resonances in the frequency band of interest [27] than the simplified model used in Fig. 2. These resonances could masquerade as a VULF DM signal; additionally they will reduce the sensitivity to the VULF DM signal in narrow bands distributed throughout the frequency range of interest. The expected VULF DM signal is narrow band, with an effective Q factor corresponding to approximately 10^6 and of strongly asymmetric shape [22]; this is much narrower than any expected mechanical resonance. Moreover, by changing the temperature of the cavity, the frequency of mechanical resonances will shift, while any VULF signal will not. Fortunately, this will allow the "baseline" sensitivity limits of Fig. 2 to be achieved across the entire bandwidth. If a signal is found to not be a mechanical resonance, it can be confirmed through the use of additional cavities. Co-located cavities could provide confirmation or rejection of the signal through phase comparisons. A network of remote cavities would provide imaging of the DM field and information about its direction of propagation.

Results.—Assuming we are limited by thermal noise as indicated in Fig. 2, we plot the search reach for ultralight scalar DM in terms of the strain h and the constraints on the electron coupling d_{m_e}, along with bounds from equivalence principle (EP) tests and other experimental data in Figs. 3 and 4, respectively. Through Eqs. (4), (2), (3), our technique is sensitive to the combination $|d_e + d_{m_e}|$; to compare with existing constraints, we assumed that d_e coupling is negligible in Fig. 4. For simplicity, we terminated the upper-frequency limit of the search range at the mechanical resonance frequency of the spacer. Several orders of magnitude of improvement beyond the limits imposed by EP and fifth-force tests [31,32] are possible at

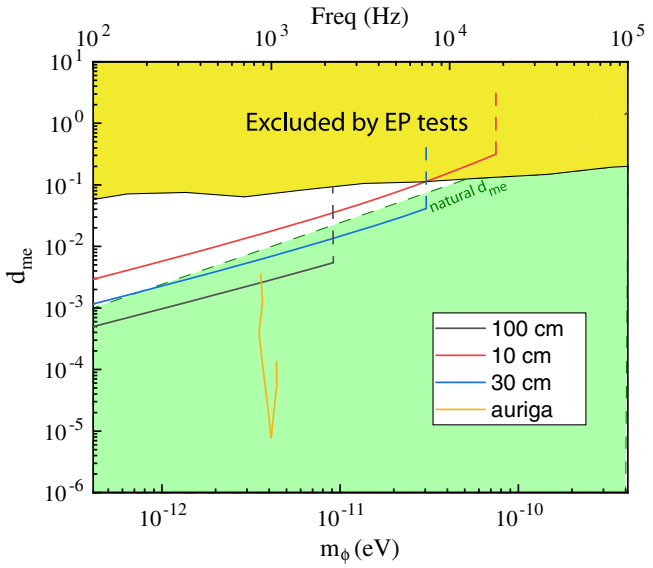

FIG. 4. Search reach for an optical cavity of length 10, 30, and 100 cm assuming thermal-noise limited sensitivity along with current experimental bounds from equivalence principle (EP) and fifth force tests [31,32] as well as the limits derived from the narrow-band AURIGA gravitational wave detector [19,33]. Also shown are natural theoretical expectations for d_{m_e} for a 10 TeV cutoff [19].

frequencies between 100 Hz and 10 kHz, depending on the length of the resonator. We also indicate the limits imposed by an analysis of the narrow-band AURIGA gravitational wave detector [19,33].

Scalar DM candidates commonly appear in string theory as moduli, and broadband sensitivity is crucial given their unknown masses. Theoretically, radiative corrections suggest a model-independent minimum mass as discussed in Refs. [6,19,20]. This naturalness criterion is satisfied inside the green bands of Figs. 3 and 4 for a hard cutoff imposed of 10 TeV. This cutoff is conservatively chosen as roughly the energy scale up to which the standard model is believed to be correct; our choice is consistent with the earlier work [19]. Thus our proposed method can begin to probe into this theoretically well-motivated region.

Discussion.—A possible extension of the proposed technique could involve operating a network of spatially separated pairs of such cavities [22]. For the VULF Compton frequency range considered here, even an intercontinental network is within the VULF coherence length. The sensitivity of the network improves as $\sqrt{N}$ with the number of nodes N. In the event of positive VULF signal discovery, a network would allow measuring the average direction for the incident DM waves. According to the standard halo model, this should point towards the Cygnus constellation. As optical cavities are commonly in use in standards laboratories worldwide, the implementation of such a network may be relatively low cost when compared with other proposed cryogenic strain-based sensing approaches [19].

While optical cavities with suspended mirrors are currently not commonly found in standards laboratories, it is common to find multiple rigid cavities of differing length, which would be sufficient to implement the proposed experiment. The DM-induced length fluctuations are suppressed above the resonant frequency of the cavity's mechanical spacer. Comparing two rigid cavities of different lengths allows the detection of a differential signal due to DM induced strain over the frequency band between the resonant frequencies of the two cavities, with the sensitivity of the shorter cavity.

Also possible is a search for "clumpy" DM composed of macroscopic objects, such as Q balls [34], that lead to transient variations of fundamental constants [35]. For these models, one may either rely on the annual variation in the measured noise non-Gaussianity for a single setup [35] or on measuring correlated propagation of variation in fundamental constants at ∼300 km/s galactic velocities through the network [4]. Prior work relating the results of axion searches to the galactic DM distribution, such as Ref. [36], could be similarly applied to the proposed observations to relate them to the galactic DM distribution.

For extending the search to higher frequency, a silicon spacer with a higher sound speed than fused silica could be used. Cryogenic silicon cavities are also a promising route to improved thermal noise performance [37], and could extend the sensitivity to VULF DM by an order of magnitude.

We would like to thank P. Hamilton, H. Muller, D. Schlippert, M. Arvanitaki, S. Dimopoulos, G. Ranjit, M. Baryakhtar, J. Huang, E. Rasel, B. Roberts, and R. Walsworth for discussions. This work was supported in part by the U.S. NSF, by the Heising-Simons Foundation, and by the National Key Research Program of China under Grant No. 2016YFA0302002, and the Strategic Priority Research Program of the Chinese Academy of Sciences under Grant No. XDB21010100.

[1] J. L. Feng, Annu. Rev. Astron. Astrophys. **48**, 495 (2010).
[2] G. Bertone, D. Hooper, and J. Silk, Phys. Rep. **405**, 279 (2005).
[3] S. Profumo, *An Introduction to Particle Dark Matter* (World Scientific, Singapore, 2017).
[4] A. Derevianko and M. Pospelov, Nat. Phys. **10**, 933 (2014).
[5] M. S. Safronova, D. Budker, D. DeMille, D. F. Jackson Kimball, A. Derevianko, and C. W. Clark, Rev. Mod. Phys. **90**, 025008 (2018).
[6] S. Dimopoulos and G. F. Giudice, Phys. Lett. B **379**, 105 (1996).
[7] N. Arkani-Hamed, L. Hall, D. Smith, and N. Weiner, Phys. Rev. D **62**, 105002 (2000).
[8] C. P. Burgess, A. Maharana, and F. Quevedo, J. High Energy Phys. 05 (2011) 10.
[9] M. Cicoli, C. P. Burgess, and F. Quevedo, J. High Energy Phys. 10 (2011) 119.
[10] T. R. Taylor and G. Veneziano, Phys. Lett. B **213**, 450 (1988).
[11] T. Damour and A. M. Polyakov, Nucl. Phys. **B423**, 532 (1994).
[12] T. Damour and J. F. Donoghue, Phys. Rev. D **82**, 084033 (2010).
[13] A. Arvanitaki, J. Huang, and K. Van Tilburg, Phys. Rev. D **91**, 015015 (2015).
[14] P. W. Graham, D. E. Kaplan, J. Mardon, S. Rajendran, and W. A. Terrano, Phys. Rev. D **93**, 075029 (2016).
[15] A. A. Geraci and A. Derevianko, Phys. Rev. Lett. **117**, 261301 (2016).
[16] D. Budker, P. W. Graham, M. Ledbetter, S. Rajendran, and A. O. Sushkov, Phys. Rev. X **4**, 021030 (2014).
[17] Y. V. Stadnik and V. V. Flambaum, Phys. Rev. Lett. **114**, 161301 (2015).
[18] Y. V. Stadnik and V. V. Flambaum, Phys. Rev. A **93**, 063630 (2016).
[19] A. Arvanitaki, S. Dimopoulos, and K. Van Tilburg, Phys. Rev. Lett. **116**, 031102 (2016).
[20] A. Arvanitaki, P. W. Graham, J. M. Hogan, S. Rajendran, and K. Van Tilburg, Phys. Rev. D **97**, 075020 (2018).
[21] R. Bradley, J. Clarke, D. Kinion, L. J. Rosenberg, K. van Bibber, S. Matsuki, M. Mück, and P. Sikivie, Rev. Mod. Phys. **75**, 777 (2003).
[22] A. Derevianko, Phys. Rev. A **97**, 042506 (2018).
[23] A. C. Melissinos, Phys. Rev. Lett. **102**, 202001 (2009).

[24] R. Drever, J. L. Hall, F. Kowalski, J. Hough, G. Ford, A. Munley, and H. Ward, Appl. Phys. B **31**, 97 (1983).
[25] Y. Hadjar, P. F. Cohadon, C. G. Aminoff, M. Pinard, and A. Heidmann, Europhys. Lett. **47**, 545 (1999).
[26] E. D. Black, A. Villar, K. Barbary, A. Bushmaker, J. Heefner, S. Kawamura, F. Kawazoe, L. Matone, S. Meidt, S. R. Rao, K. Schulz, M. Zhang, and K. G. Libbrecht, Phys. Lett. A **328**, 1 (2004).
[27] T. Chalermsongsak, F. Seifert, E. D. Hall, K. Arai, E. K. Gustafson, and R. X. Adhikari, Metrologia **52**, 17 (2015).
[28] P. R. Saulson, Phys. Rev. D **42**, 2437 (1990).
[29] A. Schroeter *et al.*, arXiv:0709.4359 [Classical Quantum Gravity (to be published)].
[30] A. V. Cumming *et al.*, Classical Quantum Gravity **29**, 035003 (2012).
[31] S. Schlamminger, K.-Y. Choi, T. A. Wagner, J. H. Gundlach, and E. G. Adelberger, Phys. Rev. Lett. **100**, 041101 (2008).
[32] T. A. Wagner, S. Schlamminger, J. H. Gundlach, and E. G. Adelberger, Classical Quantum Gravity **29**, 184002 (2012).
[33] L. Baggio, M. Bignotto, M. Bonaldi, M. Cerdonio, L. Conti, P. Falferi, N. Liguori, A. Marin, R. Mezzena, A. Ortolan, S. Poggi, G. A. Prodi, F. Salemi, G. Soranzo, L. Taffarello, G. Vedovato, A. Vinante, S. Vitale, and J. P. Zendri, Phys. Rev. Lett. **94**, 241101 (2005).
[34] A. Kusenko and P. J. Steinhardt, Phys. Rev. Lett. **87**, 141301 (2001).
[35] B. M. Roberts and A. Derevianko, arXiv:1803.00617.
[36] J. W. Foster, N. L. Rodd, and B. R. Safdi, Phys. Rev. D **97**, 123006 (2018).
[37] W. Zhang, J. M. Robinson, L. Sonderhouse, E. Oelker, C. Benko, J. L. Hall, T. Legero, D. G. Matei, F. Riehle, U. Sterr, and J. Ye, Phys. Rev. Lett. **119**, 243601 (2017).